General Disclaimer

One or more of the Following Statements may affect this Document

- This document has been reproduced from the best copy furnished by the organizational source. It is being released in the interest of making available as much information as possible.

- This document may contain data, which exceeds the sheet parameters. It was furnished in this condition by the organizational source and is the best copy available.

- This document may contain tone-on-tone or color graphs, charts and/or pictures, which have been reproduced in black and white.

- This document is paginated as submitted by the original source.

- Portions of this document are not fully legible due to the historical nature of some of the material. However, it is the best reproduction available from the original submission.

UNITED STATES DEPARTMENT OF COMMERCE
Maurice H. Stans, Secretary
NATIONAL BUREAU OF STANDARDS • A. V. Astin, Director

TECHNICAL NOTE 374

ISSUED FEBRUARY 1969

INCIPIENT AND DEVELOPED CAVITATION IN LIQUID CRYOGENS

D. K. EDMONDS AND J. HORD

Cryogenics Division
Institute for Basic Standards
National Bureau of Standards
Boulder, Colorado 80302

For sale by the Superintendent of Documents, U.S. Government Printing Office, Washington, D.C., 20402
Price 35 cents.

TABLE OF CONTENTS

List of Figures

TABLE OF CONTENTS (CONTINUED)

List of Tables

INCIPIENT AND DEVELOPED CAVITATION IN LIQUID CRYOGENS*

D. K. Edmonds and J. Hord

Cavitation characteristics of liquid hydrogen and liquid nitrogen flowing in a transparent plastic venturi have been determined and conventional cavitation-inception-parameter curves are given. Representative developed-cavitation data, consisting of pressure and temperature measurements within fully-developed cavities, are also given; measured temperatures and pressures within the cavities were generally not in thermodynamic equilibrium. Existing theory was used to obtain equations which correlate the experimental data for developed cavities in liquid hydrogen or liquid nitrogen. The theory is extended to include the effect of cavity thickness and the experimental data are used to evaluate the results. Some recommendations for future work are given.

Key words: Cavitation, cryogens, incipience

1. Introduction

Cavitation is usually categorized as gaseous or vaporous; in this paper it is also necessary to distinguish between incipient (or desinent) cavitation and fully-developed cavities. Cavitation is usually defined as the formation, caused by a reduction in pressure, of a vapor phase within a flowing liquid or at the interface between a liquid and a solid surface. For incipient cavitation, this definition is somewhat ambiguous because various criterion and methods are used to detect the vapor phase. Incipient cavitation as used herein refers to the fluid condition where the vapor phase is barely visible to the unaided eye. The visual inception criterion was chosen to conform with the bulk of the literature, and also chosen because the sensitivity [1-3]† of

* The experimental work described in this paper was performed at NBS under the sponsorship of Lewis Research Center (NASA-LeRC) under Contract No. C-35560-A.

† Numbers in brackets indicate references at the end of this paper.

various acoustic detectors can vary appreciably. An acoustic detector, which would detect cavitation in what appeared to be a pure liquid phase, was developed in the course of a recent study and is described in detail in reference [4]. Pressure and temperature profiles within fully-developed cavities were measured and are referred to herein as developed-cavitation data.

To design liquid handling equipment such as pumps and flowmeters, the designer must determine whether cavitation will occur, and in many cases, to what extent. While the non-cavitating performance of hydraulic equipment may be predicted from established similarity laws, cavitating performance can seldom be predicted from fluid to fluid. The effects of fluid properties on cavitation performance are well recognized [5-14] and require more understanding to develop improved similarity relations [15] for equipment design. NASA has undertaken a program [16] to determine the thermodynamic behavior of different fluids in an effort to obtain improved design criteria to aid in the prediction of cavitating pump performance. The experimental study described herein was conducted in support of this program. Two kinds of data are reported here: (1) cavitation inception (incipient) and (2) developed-cavitation; both are an extension of work done at NASA-LeRC, see references [15-22]. The main purpose of our experimental study [4] was to extend the experimental investigation to liquid hydrogen, and determine the scale effects of using a test section that was half the flow area of the NASA test section. Scale effects in incipient cavitation were determined by using liquid nitrogen and comparing the results with NASA nitrogen data. The purpose of the present manuscript is twofold: (1) to briefly review key experimental results of reference [4], and (2) to propose and evaluate possible improvements to existing theory regarding the effects of

fluid properties on developed-cavitation performance of equipment. The analytical part of this work extends the similarity equation [15] by permitting the cavity thickness, $\bar{t}$, to vary as a function of velocity and cavity length. The cavity thickness was taken as constant in reference [15].

The similarity equation is useful for correlating the cavitating performance [15, 16] of a particular piece of equipment from fluid to fluid; this equation is also useful in extending the velocity and temperature range of data for any given fluid. Experimental data from reference [4] were used to evaluate the postulated improvements, theory, etc., concerning this similarity equation.

2. Description of Apparatus and Operating Procedure[1]

Figure 1 is a schematic of the test apparatus, and figure 2 shows some details of the clear-plastic test section -- pressure and temperature tap locations are shown. Highly compressed elastomeric "O" rings were used to seal both faces of each of the aluminum end flanges. The entire flow system was vacuum insulated.

The operating procedure consisted of first filling the supply dewar with liquid and slowly cooling the flow system (using valves A and B -- figure 1) to the normal boiling-point temperature of the cryogen. Special attention was given to cooling the plastic test section, as it failed from thermal shock in some of the earlier tests. When the system was sufficiently cooled, the contents of the supply dewar were slowly transferred to the receiver dewar and back again in order to assure complete cooldown. The system was kept cold by maintaining

[1] See reference [4] for greater detail.

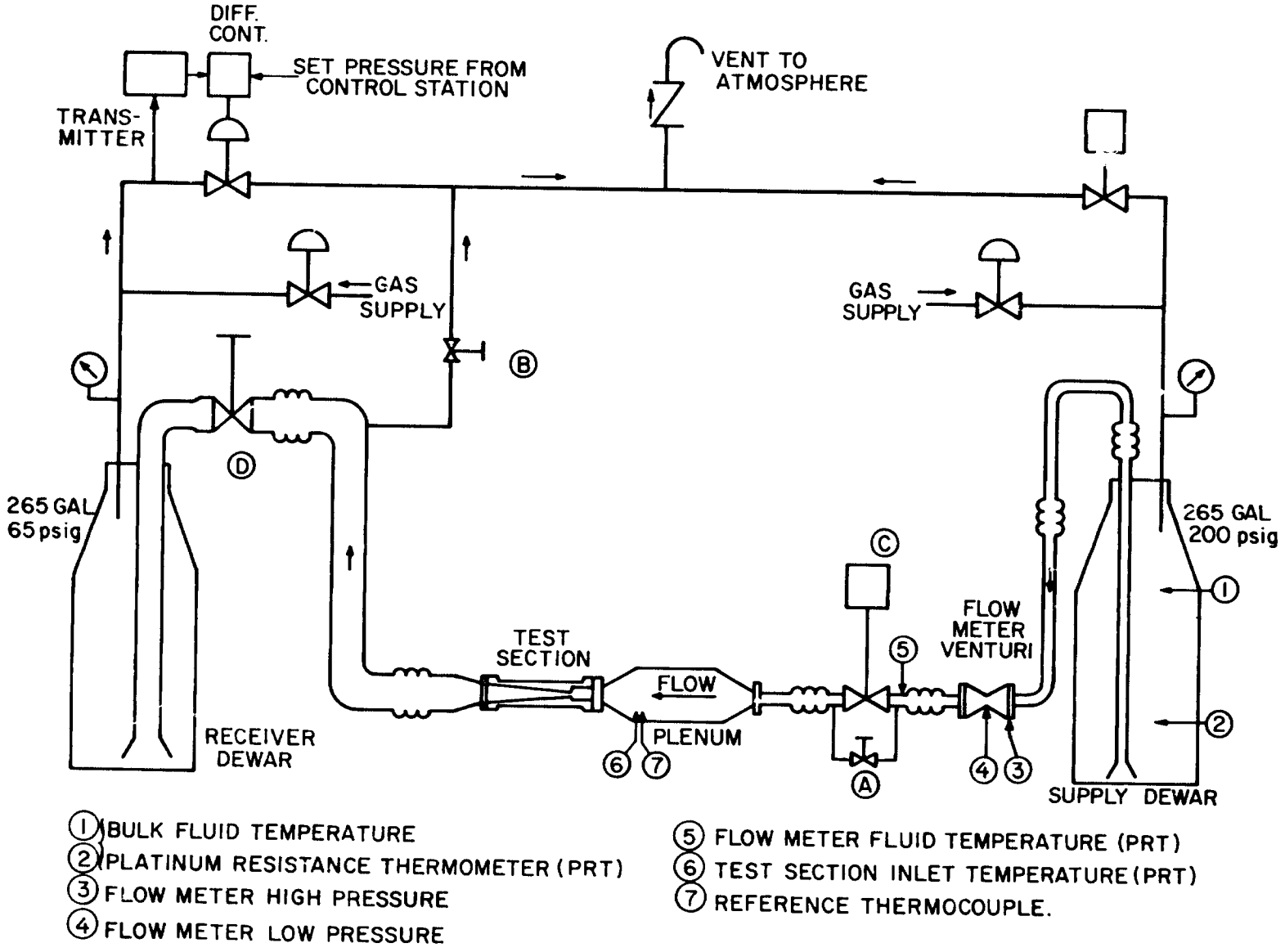

Figure 1. Schematic of cavitation flow apparatus.

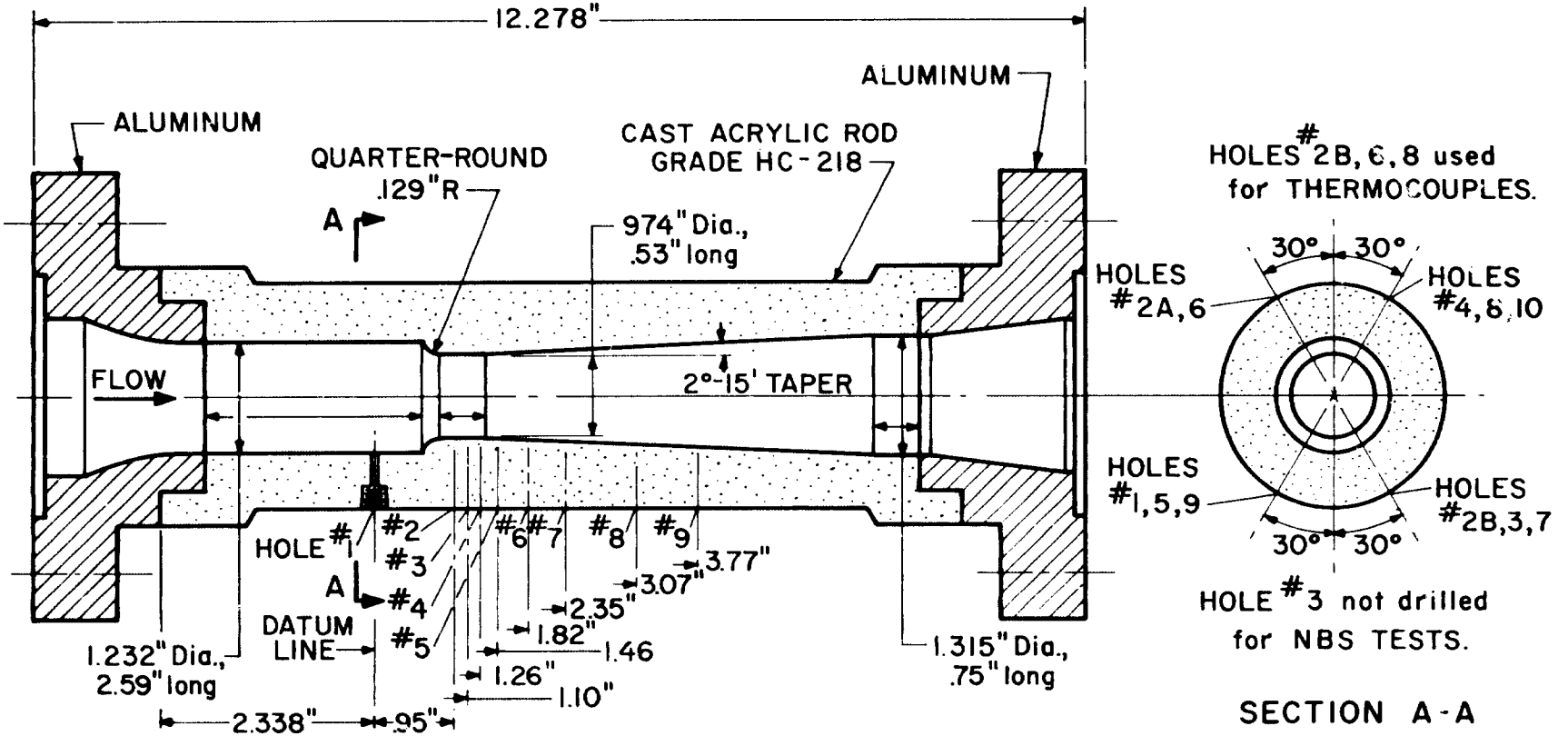

Figure 2. Detail of plastic venturi and location of pressure and temperature taps.

liquid in the test section and transfer line. Bottled gas provided the required pressure for all liquid transfers. In order to make a test, the liquid in the supply dewar was heated to the desired temperature, pressures in the supply and receiver dewars were adjusted for the desired flow conditions, and the valves (C and D) in the main flow line were then opened. Flow conditions were changed during a test by varying the receiver dewar pressure and throttling with valve D. Cavity formations in the flowing cryogens were visually monitored by focusing a closed-circuit television camera on the test section; necessary changes in flow conditions were then made to secure the desired cavitation patterns. Also, each test was recorded on 16 mm, 20 frames/sec film that was subsequently used for data reduction.

3. Instrumentation

Test fluid temperatures at the flowmeter and test section were determined by platinum resistance thermometers, see figure 1, The overall accuracy of the platinum-thermometer temperature measurement is estimated to be within ± 0.09 R. Miniature chromel-constantan thermocouples were used to determine the temperature profile within the cavities and assure rapid response during the developed-cavitation tests. The reference thermocouple was placed in the plenum chamber beside the platinum thermometer that was used to determine bulkstream temperature at the test-section inlet. The cavity temperature measurements are estimated to be accurate within ± 1 R for hydrogen and ± 0.4 R for nitrogen; the inaccuracies in these measurements are due to the low emf produced by the thermocouples at low temperatures.

System gage and differential pressure measurements were obtained with pressure transducers mounted in a temperature stabilized box near the test section. The overall accuracy of the pressure measurement, including calibration and read-out errors, is estimated to be within ± 2%. Bourdon gages were used to monitor the various tests.

Volumetric flow rates were determined by a Herschel venturi flowmeter designed to ASME standards [23]. An error analysis of this flow device and associated pressure and temperature measurements indicates the deduced mass flow should be accurate within about one percent.

An electronic pulsing circuit provided a common time base for correlating data between oscillograph, digital voltmeter (with printer), and movie film. The data were reduced by first viewing the film of the test event. A solenoid-actuated counter, installed adjacent to the test section, was energized by the electronic pulser and appears on the film. Thus, the data are reduced at the desired instant of time by simply matching the number of voltage pulses which have elapsed.

4. Discussion and Analysis of Experimental Data

Since the temperature of the cryogen changed in flowing from the supply dewar to the test section, the experimental data varied in temperature around the selected nominal temperatures. A detailed method [4] of temperature compensation was used for the incipient and desinent cavitation data. No attempt was made to separate incipient and desinent cavitation data, as both were found to occur at identical flow conditions; therefore, incipience and desinence are used synonymously in this paper. Figure 3 illustrates cavitation-parameter curves, K_{iv} versus V_o, for hydrogen. Similar data are shown on figure 4 for nitrogen. Note that the K_{iv} curves for hydrogen cross at

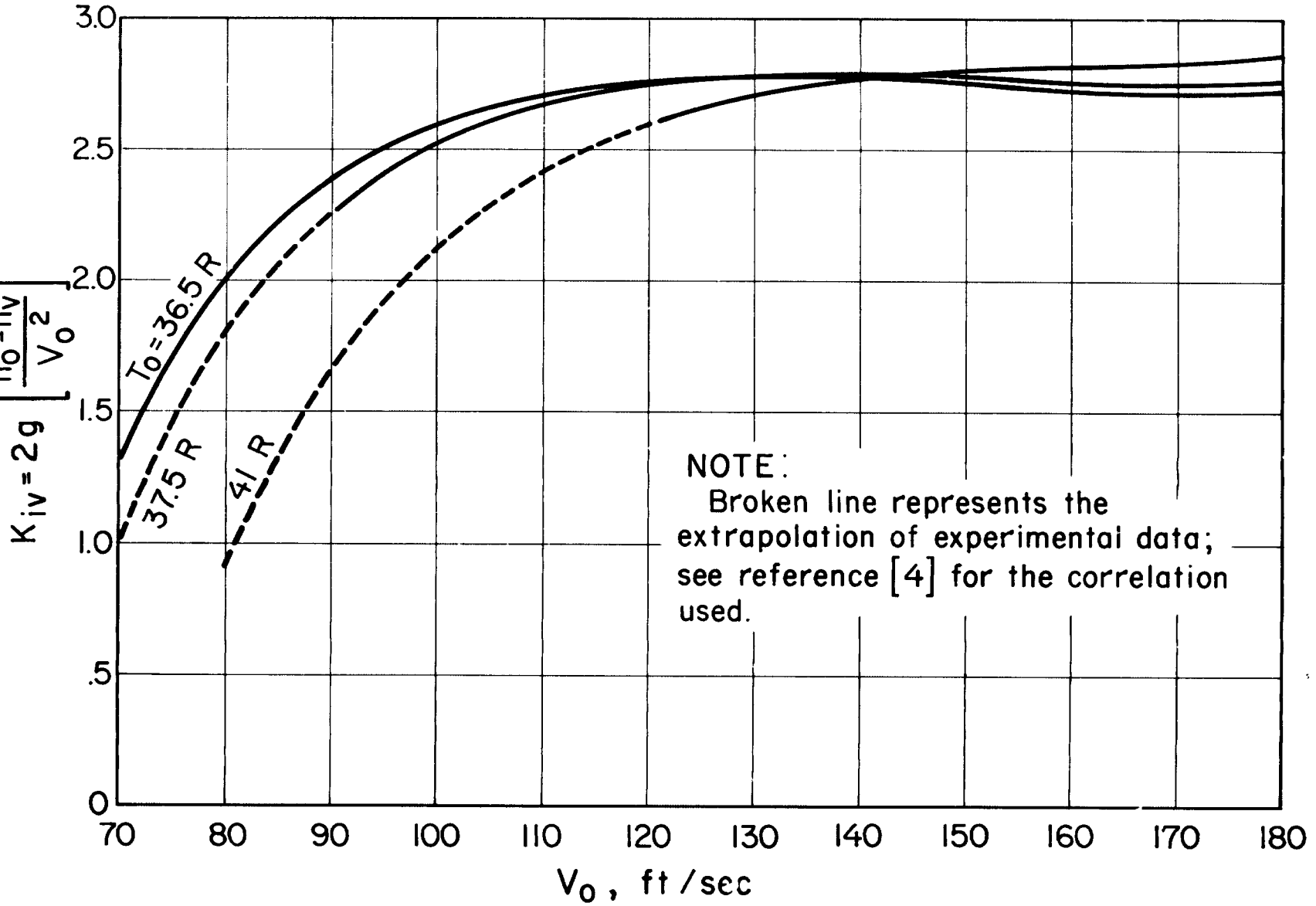

Figure 3. Incipient-cavitation parameter for liquid hydrogen as a function of test-section inlet velocity and liquid temperature.

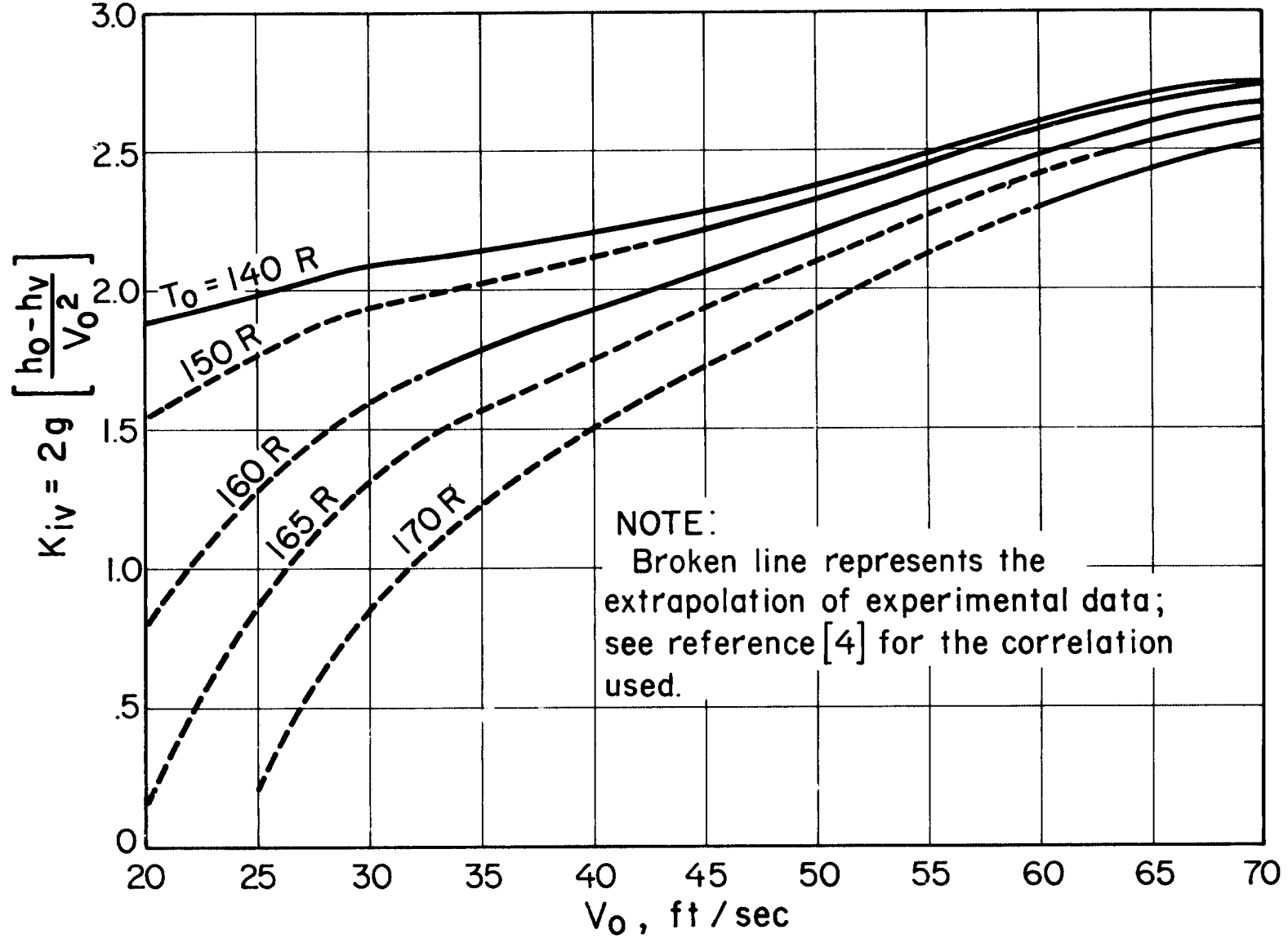

Figure 4. Incipient-cavitation parameter for liquid nitrogen as a function of test-section inlet velocity and liquid temperature.

about 140 ft/sec: intersection of these curves may be tenable; however, it is also possible that instrument error amplified in the K_{iv} parameter [4] is responsible for this behavior. The nitrogen K_{iv} curves also tend to a common value at the higher velocities. Minimum local wall pressure at incipience was calculated to be less than bulkstream vapor pressure in all of the inception tests (as much as 328 feet of hydrogen head and 63 feet of nitrogen head).

Inception data furnished by Ruggeri [18] for liquid nitrogen in a larger (1.414:1) test section were found to be coincident with the NBS [4] liquid nitrogen inception data; thus, it was concluded that the scale factor was negligible.

The developed-cavitation data did not require temperature compensation because the similarity equation compensates for variations in the temperature of the test fluid. Figure 5 presents typical[2] cavity pressure-depression curves for liquid hydrogen; figure 6 shows similar data for nitrogen. "Pressure-depression" refers to the difference between saturation pressure at inlet temperature and measured cavity pressure. Cavity temperature measurements have been converted into equivalent saturation pressures, subtracted from the bulkstream vapor pressure, and plotted on these figures for comparison with the measured pressures. This pressure-depression is plotted as a function of distance along the cavity, beginning at the minimum pressure point in the test section throat. Note that the measured pressure in the cavity is generally lower than the vapor pressure of the bulkstream liquid (in some cases [4] as much as 651 feet of hydrogen head and 44 feet of nitrogen head). In many of these

[2] More graphical and tabulated developed-cavitation data are given in reference [4].

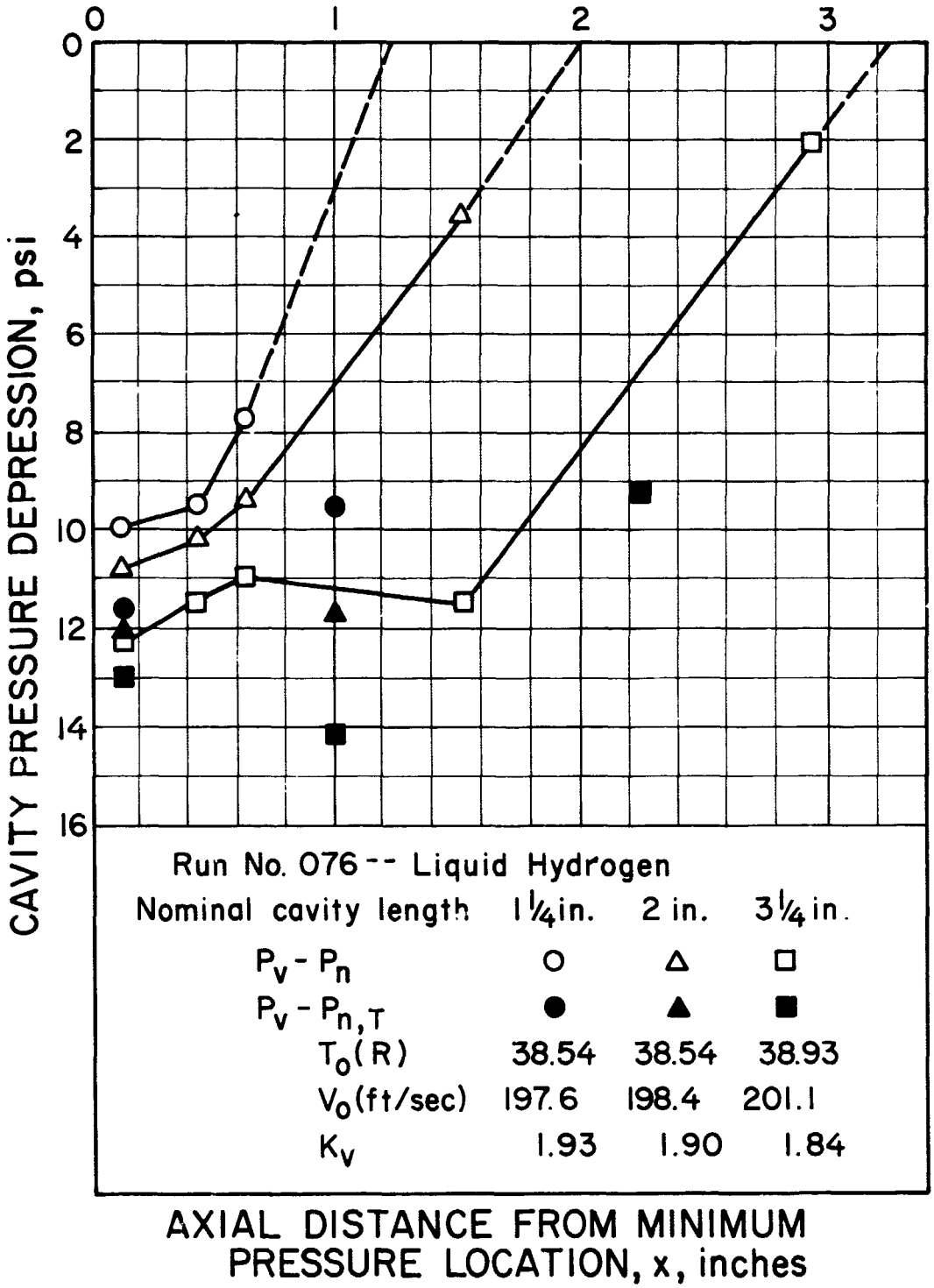

Figure 5. Typical pressure depressions within cavities in liquid hydrogen.

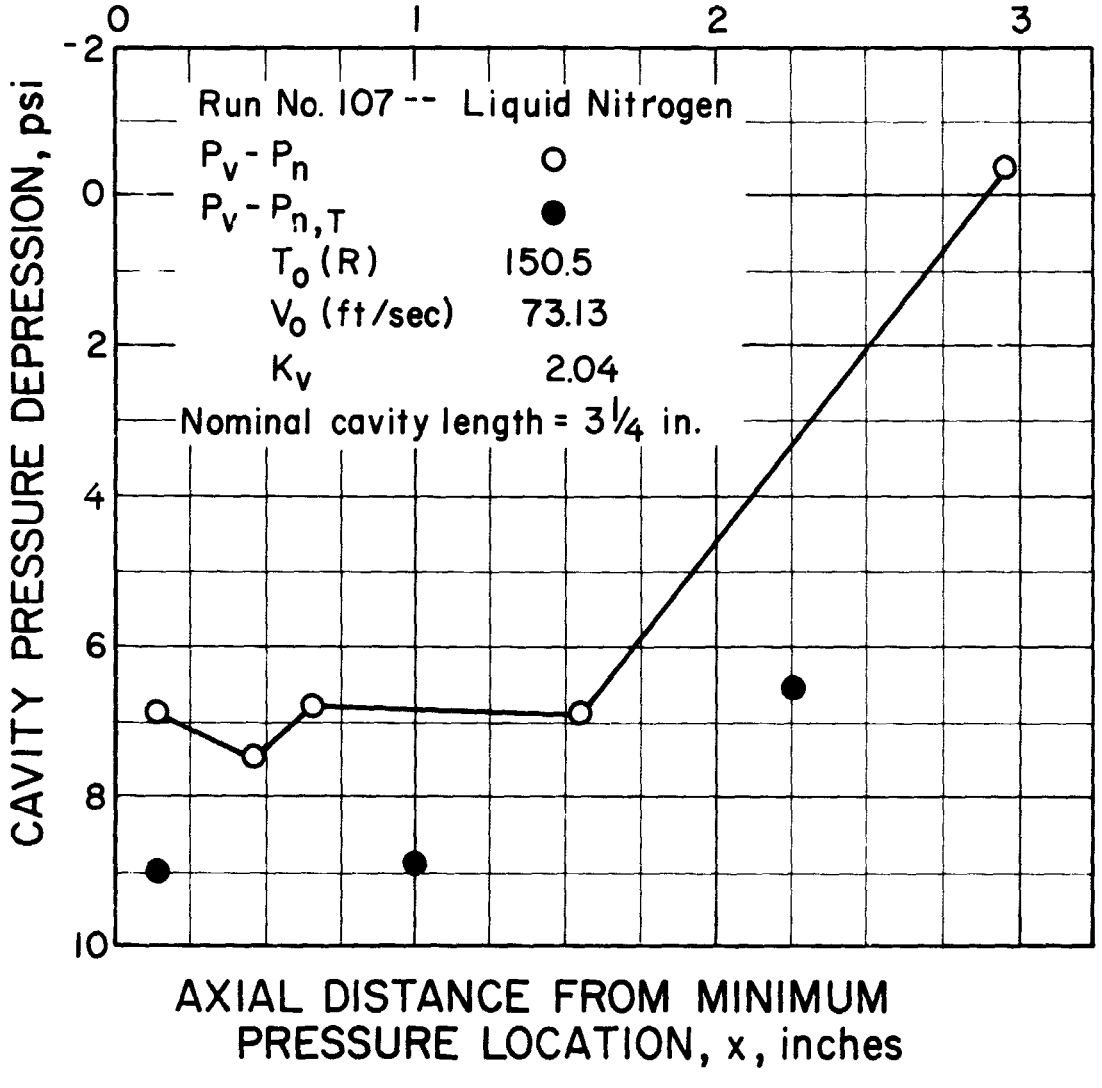

Figure 6. Typical pressure depressions within a cavity in liquid nitrogen.

developed-cavitation tests, the measured cavity pressure exceeded the saturation pressure corresponding to the measured cavity temperature by an amount which could not be attributed to errors in pressure and temperature measurements. Also, examination of the data revealed that the degree of metastability in the cavity appeared to be a function of bulkstream liquid temperature, velocity, and axial position within the cavity. It was therefore concluded that, in general, the pressures and temperatures within the cavity are not in thermodynamic equilibrium.

A series of photographs of developed-cavitation in liquid nitrogen are shown in figure 7; the porosity of the nitrogen cavities usually decreases with increasing velocity or increasing temperature. These photographs are representative of conditions at which data were reduced. Similar photographs of hydrogen cavities are not shown because the cavities are nonporous and uniform in structure, see reference [4].

5. Extension of the Cavitation Similarity-Equation Theory[3]

The similarity equation for developed-cavitation is given in reference [15] as follows:

$$B = B_{ref}\left[\left(\frac{\alpha_{ref}}{\alpha}\right)\left(\frac{\ell_{ref}}{\ell}\right)\left(\frac{V_o}{V_{o,ref}}\right)\right]^{0.5}\left(\frac{\bar{t}}{\bar{t}_{ref}}\right). \qquad (1)$$

The symbols are identified in the nomenclature section of this paper; B is the volume of vapor in the cavity divided by the volume of liquid

[3] Applications of the similarity equation are described in the introduction to this paper, see references [15, 16, 24].

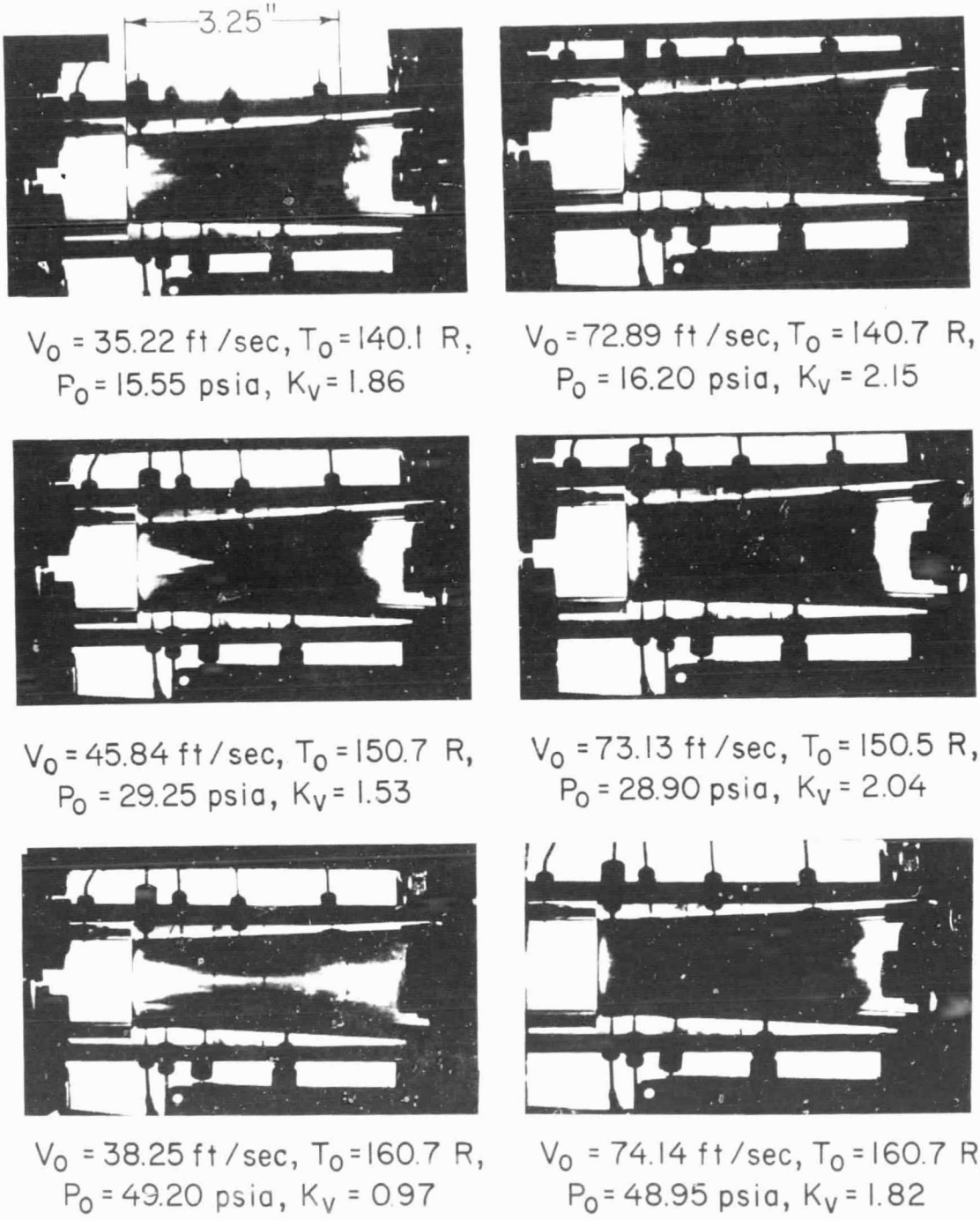

Figure 7. Photographs showing effects of velocity and temperature on the appearance of developed cavities in liquid nitrogen; nominal cavity length, 3.25 in.

from which heat has been extracted (due to vaporization) in forming the cavity. B can also be obtained from a theoretical expression relating cavity pressure-depression to "B" factor; this theoretical value is called B_t. The B_t is derived from an energy balance between the vapor and the cooled liquid film at the liquid-vapor interface. The main assumptions used to derive B_t have been attributed to several authors (see ref. [14]) and are summarized in reference [15]. For purposes of calculation, the numerical value of B_t can be obtained from 1) fluid properties and 2) the expression for B_t given in reference [15].

To account for the difference between theory and practice, equation (1) can be written in the following form,

$$B = B_{ref} \left(\frac{\alpha_{ref}}{\alpha}\right)^m \left(\frac{\ell_{ref}}{\ell}\right)^n \left(\frac{V_o}{V_{o,ref}}\right)^p \left(\frac{\bar{t}}{\bar{t}_{ref}}\right) . \qquad (2)$$

The exponents in equation (2) are evaluated from experimental data as follows:

(1) B_t is obtained for each experimental data point from a cavity pressure-depression $(P_v - P_n)$ versus "B" factor plot, see reference [15].

(2) One data point is arbitrarily chosen as a "reference"; the α, ℓ, V_o, and B_t from the chosen experimental run are then inserted into equation (2) as constants where the subscript "ref" occurs. The $\bar{t}$ term can be considered equal to unity (as in previous studies [4, 15]) or a function of cavity length, ℓ, and velocity, V_o (see discussion below); in the latter case, the $\bar{t}$ term is absorbed into the ℓ and V_o terms.

(3) Values of α, ℓ, and V_o from each data point are then inserted into equation (2) as the non-subscripted terms. This produces an equation for every data point except the one chosen as a reference. Note that the unknowns in this set of simultaneous equations are B and the exponents m, n, and p.

(4) The computer is then programmed to range through values of the exponents — one at a time. For each new value of m, n, or p the computer finds the value for B, on the left side of equation (2), then computes the sum of the squares of the differences between the calculated B and the B_t for each equation. The computer adjusts the exponents until the sum of the squares of the differences are minimized; in some cases, one or more exponents were held constant at theoretical or arbitrary values. This process ensures that the calculated B values are brought as closely as possible to their respective theoretical B_t values; the exponents computed in this manner represent the best agreement between experiment, equation (2), and the energy balance equation for B_t.

In the work of Gelder, et al. [15], the cavity thickness ratio in equation (2) was assumed to be unity and the exponents for the other terms were experimentally evaluated. The exponents obtained by Gelder, et al. for F-114, along with the theoretical exponents, equation (1), were applied to the data obtained in recent NBS experiments [4]. The "best fit" set of exponents were also obtained by computer for these data, again assuming the $\bar{t}$ term equal to unity. Tables of exponents, along with their standard deviations in the B factor, are given in table 1 for hydrogen and table 2 for nitrogen. The standard deviation is a measure of the validity of the theories for the similarity and B_t expressions as both are evaluated from

Table 1: Evaluation of Similarity Equation Using Liquid Hydrogen Data.

Data Identification	Source of Exponents (i.e., assumed cavity shapes from this paper and exponents obtained from reference material.)		Exponents‡			Standard Deviations† Using reference cavity lengths as follows:		
			m	n	p	1.25 in.	2.00 in.	3.25 in.
T 1-1	Theory [15]; See equation (1).	$\bar{t} = \bar{t}_{ref}$	.5	.5	.5	1.64	1.36	2.22
T 1-2	Gelder, et al. [15], experimental data with F-114.		.5	-.16	.85	.83	.92	.67
T 1-3	NBS Seek-Fit		.5	.5	.314*		1.33	
T 1-4			.5	-.278*	.5			.58
T 1-5			.5	-.332*	.5		.58	
T 1-6			.5	-.372*	.5	.56		
T 1-7			.5	-.308*	.732*			.56
T 1-8			.5	-.348*	.446*		.57	
T 1-9			.5	-.39*	.61*	.56		
T 1-10			-3.52*	-.348*	.554*			.38
T 1-11			-3.82*	-.304*	.644*		.36	
T 1-12			-3.82*	-.414*	.496*	.41		
T 1-13			-4.62*	.5	.5		1.17	
T 1-14	Exponents chosen as a compromise between theory and experiment	$\bar{t} = \bar{t}_{ref}$	.5	-.3	.5	.59	.58	.58
T 1-15	Semi-cubical parabola	$t^3 = kx^2$	.5	-.167	.5	.74	.63	.62
T 1-16	Concave parabola	$t^2 = kx$	.5	0	.5	.98	.76	.84
T 1-17	Straight line	$t = kx$	.5	-.5	.5	.66	.63	.71
T 1-18	Semi-cubical parabola	$t^3 = kV_o x^2$	.5	-.167	.833	.82	.89	.65
T 1-19	Concave parabola	$t^2 = kV_o x$	.5	0	1.0	1.11	1.23	.99
T 1-20	Straight line	$t = kV_o x$	.5	-.5	1.5	.77	2.49	.78

‡ $B = B_{ref} \left(\frac{\bar{\ell}_{ref}}{\bar{\ell}}\right)^m \left(\frac{\bar{t}_{ref}}{\bar{t}}\right)^n \left(\frac{V_o}{V_{o,ref}}\right)^p$.

† Standard Deviation = $\sqrt{[\Sigma(B-B_t)^2]/N}$ where N = number of data points, B_t is computed from theory [15], and B is computed from equation (2).

* Exponents selected by computer, from experimental data, using a "least squares" fitting technique.

Table 2: Evaluation of Similarity Equation Using Liquid Nitrogen Data.

Data Identification	Source of Exponents		Exponents‡		Standard Deviations† using 3.25 inch cavity as reference.
			m	p	
T 2-1	Theory [15]; see equation (1).	$\bar{t} = \bar{t}_{ref}$	.5	.5	.545
T 2-2	Gelder, et al.[15] experimental data with F-114	↓	.5	.85	.671
T 2-3	NBS seek-fit		.5	.385*	.533
T 2-4	"		-1.22*	.492*	.498

‡ $B = B_{ref} \left(\frac{\alpha_{ref}}{\alpha}\right)^m \left(\frac{V_o}{V_{o,ref}}\right)^p$.

† Standard Deviation = $\sqrt{[\Sigma(B - B_t)^2]/N}$ where N = number of data points, B_t is computed from theory [15], and B is computed from equation (2).

* Exponents selected by computer, from experimental data, using a "least squares" fitting technique.

experimental data. The numerical value of B_t usually lies between two and five.

Because the "best fit" exponents vary appreciably from the theoretical values, one possibility for improvement is to let $\bar{t}$ be a function of cavity length and velocity. As an example, assume that the cavity has the shape of a semi-cubical parabola, $t^3 = ax^2$; if we also assume that the coordinate proportionality factor is linearly related to V_o, then $a = kV_o$ where k is constant for any given fluid and test item. Obtaining the expression for $\bar{t}$ requires an integration:

$$\bar{t} = \frac{1}{\ell} \int_o^{\ell} (kV_o)^{1/3} x^{2/3} dx. \qquad (3)$$

Integration of equation (3) and substitution of the resulting $\bar{t}$ into equation (1) produces the following:

$$B = B_{ref} \left(\frac{\alpha_{ref}}{\alpha}\right)^{0.5} \left(\frac{\ell_{ref}}{\ell}\right)^{-0.167} \left(\frac{V_o}{V_{o,ref}}\right)^{0.833} \left(\frac{k}{k_{ref}}\right)^{0.333}. \qquad (4)$$

The $(k/k_{ref})^{0.333}$ term is taken as unity because the similarity equation requires geometrically similar cavity shapes from fluid to fluid for a specific test item; also, correlations[4] between fluids are not being evaluated here and

---

[4] Limited nitrogen data precluded correlation between nitrogen and hydrogen fluids, and NASA-LeRC personnel are preparing computer correlations [25] using available hydrogen and F-114 data.

$$B = B_{ref}\left(\frac{\alpha_{ref}}{\alpha}\right)^{0.5}\left(\frac{\ell_{ref}}{\ell}\right)^{-0.167}\left(\frac{V_o}{V_{o,ref}}\right)^{0.833} \qquad (5)$$

Other basic geometrical cavity shapes can be assumed and different exponents for the ℓ and V_o terms will result. Table 1 lists the standard deviation in B factor resulting from use of several assumed cavity shapes, as applied to the liquid hydrogen cavitation data obtained from recent experiments. The cavity thickness may also be treated as a function of cavity length, but independent of velocity. In this case $t^q = kx^w$, and q and w depend only upon the assumed cavity geometry; e.g., $q = w = 1$ for a straight-line variation, etc. Computer results for some basic cavity shapes (neglecting effect of velocity on cavity thickness) are also given in table 1.

6. Discussion of Results Given in Tables 1 and 2

Developed-cavitation data for nitrogen were obtained for one cavity length only; therefore, the postulations concerning cavity shape could only be applied to the hydrogen data where three cavity lengths were available. Examination of table 1 shows that the basic theory (data set T1-1) gives rather poor results in terms of the standard deviation: better results are obtained by using the exponents of Gelder, et al., (data set T1-2) or by permitting the computer to select one or more of the exponents (T1-3 through T1-13); of course, the "best fit" exponents in sets T1-10 through T1-12 give the best results[5].

[5] Standard deviation is minimized in those computations where one or more exponents are selected by the computer; the absolute minimum standard deviation is obtained by permitting the computer to select all three exponents.

In table 1, three different cavity lengths were used as references in order to determine the effect of reference length upon standard deviation. The exponents $m = 0.5$, $n = -0.3$, and $p = 0.5$ (see data set T1-14) were least affected by reference cavity length; note that these exponents produce a low standard deviation. In general, the 2.0 in. and 3.25 in. cavities provided the lowest standard deviations. Note that the exponent p is theoretically 0.5 for all cavity shapes assumed to be independent of velocity (T1-15, T1-16 and T1-17); also p tends to 0.5 when all three exponents are allowed to seek a best fit (T1-10, T1-11 and T1-12 for hydrogen; T2-4 for nitrogen).

Table 1 shows that velocity-dependent cavity shapes (T1-18, T1-19 and T1-20) produce standard deviations that exceed those for cavity shapes where velocity is neglected (T1-15, T1-16 and T1-17). However, the semi-cubical parabola with a velocity-dependent shape (T1-18) does give almost the same exponents that Gelder, et al., obtained (T1-2) with F-114. Perhaps the concept of velocity-dependent cavity shape is pertinent for some fluids other than hydrogen. The assumption that average cavity thickness is a function of cavity length indicates considerable promise for hydrogen; the semi-cubical parabola (T1-15) and the straight line (T1-17) shapes give the best results of the three cavity shapes examined here.

The lack of variation in $\alpha (< 10\%)$ may explain why the exponent m tends to a negative number in a seek fit (T1-10 through T1-13 for hydrogen and T2-4 for nitrogen); because the standard deviation is barely affected by this small variation in α, m was usually held at the theoretical value of 0.5.

7. Summary

1) Incipient-cavitation-parameter curves are given for liquid hydrogen in the ranges of 36.5 to 41 R and up to 180 ft/sec, and for liquid nitrogen in the ranges of 140 to 170 R and 20 to 70 ft/sec. A comparison of this liquid nitrogen incipient-cavitation data with nitrogen data obtained by NASA indicated negligible scale effects. Bulkstream vapor pressure exceeded the calculated minimum local wall pressure in all of the incipient cavitation tests.

2) Some characteristic data for developed-cavitation in both hydrogen and nitrogen are given in the form of pressure-depression curves. These curves show that the pressure and temperature in the cavity are generally not in thermodynamic equilibrium.

3) Recent NBS data are used to analyze and evaluate the basic similarity-equation theory and to compare these results with the experimental work of others; the cavity thickness ratio is assumed to be unity, see tables 1 and 2.

4) An analytical method, to account for variations in cavity thickness, is proposed and evaluated using the NBS hydrogen data; the results are again compared with the experimental work of others, see table 1. The proposed method holds some promise for improvement of the cavitation similarity equation.

8. Recommendations for Future Work

1) More developed-cavitation data, using closely spaced pressure and temperature taps, is needed to ascertain more precisely the cavity pressure profile and fluid metastability.

2) All existing developed-cavitation data, including Gelder, et al. [15], should be computer correlated in order to determine the pertinency of assumptions concerning cavity shape; these correlations would use the existing "static-model" theory.

3) Experiments should be designed to indicate the general shape of the cavity, thereby putting the theory on a firmer basis.

4) An analysis should be performed to redevelop the cavity model, accounting for dynamic effects. Existing data could be used to evaluate the results of this analysis.

9. Nomenclature

a	=	coordinate proportionality factor in cavity shape equations
B	=	ratio of vapor to liquid volume associated with the formation and sustenance of a fixed cavity in a liquid
g	=	gravitational acceleration, local, given in engineering units as $g = 32.2$ ft/sec^2
h_o	=	test section inlet head corresponding to absolute inlet pressure, ft
h_v	=	head corresponding to saturation pressure at the test section inlet temperature, ft
k	=	constant used in expression for cavity thickness t
K_{iv}	=	incipient cavitation parameter $[\equiv (h_o - h_v)/(V_o^2/2g)]$
K_v	=	fully-developed cavitation parameter $[\equiv (h_o - h_v)/(V_o^2/2g)]$
ℓ	=	total cavity length measured from minimum-pressure point on quarter-round contour along axis of plastic venturi

P_n	=	(n = 2, 4, 5, 7, or 9): absolute cavity pressure measured at a particular station or instrument port in wall of plastic venturi
$P_{n, T}$	=	(n = 2, 6, or 8): saturation pressure corresponding to the measured cavity temperature at a particular station or instrument port in wall of plastic venturi
P_o	=	test section absolute inlet pressure
P_v	=	saturation pressure at test section inlet temperature
t	=	local thickness of vapor-filled cavity at any x value
$\bar{t}$	=	average thickness of vapor-filled cavity
T_o	=	bulkstream temperature, in degrees Rankine, of liquid entering the test section
V_o	=	velocity of liquid at inlet to test section
x	=	distance measured from minimum-pressure point on quarter-round contour along axis of plastic venturi (The minimum pressure point is located on the quarter-round at 24 degrees of arc measured from the point of tangency between quarter-round and venturi throat)

Greek

α	=	thermal diffusivity of liquid

Subscripts

ref	=	reference test, or set of test conditions, to which a computation is being referenced when attempting to correlate cavitation performance via the similarity equation (1)
t	=	denotes theoretical origin

Superscripts

m	=	exponent of thermal-diffusivity ratio in equation (2)
n	=	exponent of cavity-length ratio in equation (2)
p	=	exponent of test-section-inlet-velocity ratio in equation (2)
q	=	exponent in expression for cavity thickness
w	=	exponent in expression for cavity thickness

10. References

1. C. P. Kittredge, "Detection and Location of Cavitation", Rept. MATT-142, Plasma Physics Lab., Princeton Univ., Princeton, N. J. (1962). Available from the Clearinghouse for Federal and Scientific Technical Information, Springfield, Va.

2. A. F. Lehman and J. O. Young, "Experimental Investigations of Incipient and Desinent Cavitation", ASME Journ. of Basic Eng., 86: 275 (1964).

3. J. W. Holl (ed.), "Discussions - Symposium on Cavitation Research Facilities and Techniques", Presented at Fluids Eng. Div. Conf. (Phila., Pa., May 18-20, 1964). Available from ASME, United Eng. Center, 345 East 47th St., New York 17, N. Y.

4. J. Hord, D. K. Edmonds, and D. R. Millhiser, "Thermodynamic Depressions Within Cavities and Cavitation Inception in Liquid Hydrogen and Liquid Nitrogen", NASA Rept. CR-72286, (1968). Available from NASA, Office of Scientific and Technical Information, AFSS-A, Wash., D. C.

5. J. Hord, R. B. Jacobs, C. C. Robinson and L. L. Sparks, "Nucleation Characteristics of Static Liquid Nitrogen and Liquid Hydrogen", ASME Journ. of Eng. for Power, 86: 485 (1964).

6. R. S. Brand, "The Motion of a Plane Evaporation Front in a Superheated Liquid", Tech. Rept. No. 2, Univ. of Conn., Storrs, Conn. (1963).

7. J. A. Clark, "The Thermodynamics of Bubbles", Tech. Rept. No. 7, Mass. Inst. of Tech., Cambridge 39, Mass. (1956).

8. J. W. Holl and G. F. Wislicenus, "Scale Effects on Cavitation", ASME Journ. of Basic Eng., 83: 385 (1961).

9. M. C. Huppert, W. S. King, and L. B. Stripling, "Some Cavitation Problems in Rocket Propellant Pumps", Rocketdyne Rept., Rocketdyne, Canoga Park, Calif. Presented at ASME Confer, Houston, Texas (1959).

10. V. Ya. Karelin, "Cavitation Phenomena in Centrifugal and Axial Pumps", NASA accession no. N66-14532, (1963). Available from Scientific and Technical Information Facility, P.O. Box 33, College Park, Md., (consists of 128 pages).

11. W. A. Spraker, "The Effects of Fluid Properties on Cavitation in Centrifugal Pumps' ASME Journ. of Eng. for Power, 87: 309 (1965).

12. A. J. Stepanoff, "Cavitation Properties of Liquids", ASME Journ. of Eng. for Power, 86: 195 (1964).

13. W. W. Wilcox, P. R. Meng, and R. L. Davis, "Performance of an Inducer-Impeller Combination at or Near Boiling Conditions for Liquid Hydrogen", in: K. D. Timmerhaus (ed.), Advances in Cryogenic Engineering, Vol. 8, Plenum Press, New York (1963), p. 446.

14. A. Hollander, "Thermodynamic Aspects of Cavitation in Centrifugal Pumps", ARS Journ., 32: 1594 (1962).

15. T. F. Gelder, R. S. Ruggeri, and R. D. Moore, "Cavitation Similarity Considerations Based on Measured Pressure and Temperature Depressions in Cavitated Regions of Freon 114", NASA TN D-3509 (1966).

16. I. I. Pinkel, M. J. Hartmann, C. H. Hauser, M. J. Miller, R. S. Ruggeri, and R. F. Soltis, "Pump Technology", NASA accession no. N66-33672, (1966). Available from Scientific and Technical Information Facility, P.O. Box 33, College Park, Md., (consists of 20 pages).

17. R. S. Ruggeri and T. F. Gelder, "Cavitation and Effective Liquid Tension of Nitrogen in a Hydrodynamic Cryogenic Tunnel", in: K. D. Timmerhaus (ed.), Advances in Cryogenic Engineering, Vol. 9, Plenum Press, New York (1964), p. 304.

18. R. S. Ruggeri, private communication to the authors.

19. R. S. Ruggeri, R. D. Moore, and T. F. Gelder, "Incipient Cavitation of Ethylene Glycol in a Tunnel Venturi", NASA TN D-2772, (1965).

20. R. S. Ruggeri and T. F. Gelder, "Effects of Air Content and Water Purity on Liquid Tension at Incipient Cavitation in Venturi Flow", NASA TN D-1459, (1963).

21. R. S. Ruggeri and T. F. Gelder, "Cavitation and Effective Liquid Tension of Nitrogen in a Tunnel Venturi", NASA TN-2088 (1964).

22. T. F. Gelder, R. D. Moore, and R. S. Ruggeri, "Incipient Cavitation of Freon - 114 in a Tunnel Venturi", NASA TN D-2662 (1965).

23. Flow Measurement, Chap. 4, Part 5, ASME, 29 West 39th St., New York 18, (1959), p. 17.

24. R. S. Ruggeri and R. D. Moore, "Method for Prediction of Pump Cavitation Performance in Various Liquids", to be published.

25. R. D. Moore and R. S. Ruggeri, "The Prediction of Thermodynamic Effects of Developed Cavitation Based on Liquid Hydrogen and Freon - 114 Data in Scaled Venturis", to be published.

GPO 848-757